

REAL-TIME SPECKLE INTERFEROGRAM ANALYSIS AND ITS APPLICATION TO SUB-SURFACE DELAMINATION CRACK DETECTION IN CARBON FIBRE COMPOSITES

J. M. Huntley, C. R. Coggrave and Y. Shen

Department of Mechanical Engineering, Loughborough University,
Loughborough LE11 3TU, UK

ABSTRACT

A real-time system for analysing data from speckle interferometers, and speckle shearing interferometers, has been developed. Interferograms are continuously recorded by a CCD camera at a rate of 60 frames s⁻¹ with temporal phase shifting carried out at the same rate. The images are analysed using a pipeline image processor. With a standard 4-frame phase-shifting algorithm (phase steps of $\pi/2$), wrapped phase maps are calculated and displayed at 15 frames s⁻¹. These are unwrapped using a temporal phase unwrapping algorithm to provide a real-time display of the relevant displacement component. The main advantage of temporal over spatial unwrapping methods is that unwrapping errors due to noise, specimen boundaries, and cracks do not propagate spatially. Each camera pixel (or cluster of pixels) behaves in effect as an independent displacement sensor. The reference speckle interferogram is updated automatically at regular user-defined intervals, allowing arbitrarily large deformations to be measured and errors due to speckle decorrelation to be minimized. The system has been applied to the problem of detecting sub-surface delamination cracks in carbon fibre composite panels.

KEYWORDS

Speckle interferometry, delamination cracks, defect detection, carbon fibre composites.

INTRODUCTION

The detection of delamination defects within composite structures is an important quality control step in the aerospace manufacturing industry. The traditional technique (ultrasound C-scan) is effective, but since it is a pointwise method, assessment of an entire aircraft is a time consuming and expensive process. The use of wholefield optical techniques, such as speckle interferometry and speckle shearing interferometry (shearography), is therefore potentially attractive. Electronic speckle pattern interferometry (ESPI) refers to the technique of generating fringe patterns on a TV monitor, by the real-time analysis of laser speckle interference patterns from objects with rough surfaces [1]. Traditional ESPI systems subtract a stored reference speckle pattern from the live camera image and display the modulus of the difference pattern. Systems have been constructed more recently in which further real-time data analysis is carried out using specialised pipeline image processors. By introducing phase-shifting devices, fringes with improved signal-to-noise ratio can be produced [2], or else wrapped phase maps (i.e., phase values lying in the range $-\pi$ to π) can be calculated in real time [3].

The drawback with such systems is that the calculated data are still not in the form of displacement or strain fields that can be readily understood by likely end users of the equipment. The normal method of obtaining such images is to post-process discrete “snapshots” of the wrapped phase change distribution, using the process known as phase unwrapping. The traditional method, which can be termed spatial unwrapping, involves comparing the phase at neighbouring pixels and adding suitable integral multiples of 2π so as to remove the 2π phase jumps. When the object contains real discontinuities, however, due for example to specimen edges or growing cracks, spatial unwrapping is risky because of the possibility of unwrapping across a boundary which can cause the spatial propagation of a large phase error. A wide variety of algorithms has been proposed over the years [4], but many of these are also computationally intensive, and have variable run times.

One solution to these problems is to analyse a sequence of interferograms measured throughout the entire deformation history. If the temporal sampling rate is sufficiently high, temporal phase shifting can be used to extract high quality phase maps, and temporal phase unwrapping allows absolute displacement fields to be obtained [5]. Absolute in this context means the total displacement since the start of the deformation process, as opposed to the displacement relative to some other point in the field of view, which is all that can be achieved with spatial unwrapping. The combination of temporal phase shifting and temporal phase unwrapping means that each pixel in the camera behaves as an independent displacement sensor. Several practical systems based on this approach have now been developed [6-8]. However, all of these involve storing the interferograms in memory and require subsequent post-processing.

The purpose of this paper is to describe a novel analysis system, suitable for use with either a speckle interferometer or shearography head, in which both the temporal phase shifting and temporal unwrapping calculations are carried out in real time. The result is a continuous colour-coded display of the displacement (or displacement-gradient) field which is updated at 15 Hz. The paper is illustrated with typical results from vacuum-loading experiments on a carbon fibre panel containing a simulated delamination crack.

DATA ANALYSIS

In this section we present a summary of the main numerical procedures described in References [5] and [8]. The measured intensity $I(t)$ at a given camera pixel follows the usual phase-shifting interferometry equation

$$I_n(t) = I_r + I_o + 2\sqrt{I_r I_o} \cos[\Phi(t) + \phi_n], \quad [\phi_n = (n-1)\pi/2, \quad n = 1, 2, 3, 4], \quad (1)$$

where I_r and I_o are the reference and object beam intensities, t is the time index for the phase calculation ($t = 0, 1, 2, \dots, s$), and $\Phi(t)$ is the speckle phase. ϕ_n is the phase shift which is introduced by means of a Pockels cell in the reference beam. Application of the standard 4-frame phase-shifting algorithm allows the change in phase Φ between times t_1 and t_2 to be calculated as

$$\Delta\Phi_w(t_2, t_1) = \tan^{-1} \left[\frac{N(t_2)D(t_1) - N(t_1)D(t_2)}{N(t_1)N(t_2) + D(t_1)D(t_2)} \right], \quad (2)$$

where the numerator $N(t)$ and denominator $D(t)$, respectively proportional to $\sin[\Phi(t)]$ and $\cos[\Phi(t)]$, are given by

$$N(t) = I_4(t) - I_2(t), \quad D(t) = I_1(t) - I_3(t). \quad (3)$$

Subscript w indicates that $\Delta\Phi_w(t_2, t_1)$ is wrapped onto the range $(-\pi, \pi)$.

In Eqn. (2), the numerator and denominator are proportional to the sine and cosine of the phase change between times t_1 and t_2 , weighted by the square of the intensity modulation. Spatial smoothing can therefore be carried out by convolving the numerator and denominator with a kernel of equal constant values over data from neighbouring pixels, and it can be shown that the implicit weighting results in a phase-difference map with optimal signal-to-noise ratio [9]. Such an approach has been implemented on the pipeline image processor using a 3 by 3 kernel.

Eqn. (2) allows $\Delta\Phi_w(t,0)$, the total wrapped phase change since the start of the recording process, to be calculated. Temporal phase unwrapping is then carried out to restore the unknown integral multiple of 2π for each value of t . The unwrapped phase change distribution will be denoted $\Delta\Phi_u(t,0)$. The number of 2π phase jumps between two successive measurements of the phase change is calculated as follows:

$$d(t) = \text{NINT} \left\{ \Delta\Phi_w(t,0) - \Delta\Phi_w(t-1,0) \right\} / 2\pi, \quad t = 2, 3, \dots, s, \quad (4)$$

where NINT denotes rounding to the nearest integer.

The total number of phase jumps by the time of the t th phase measurement, $v(t)$, is calculated by

$$v(t) = \sum_{t'=2}^t d(t'). \quad (5)$$

and the unwrapped phase difference map is obtained as

$$\Delta\Phi_u(t,0) = \Delta\Phi_w(t,0) - 2\pi v(t) \quad t = 2, 3, \dots, s. \quad (6)$$

If the deformation becomes too large, significant speckle decorrelation will occur causing an increase in the noise level of the measured displacement fields. Under such circumstances a new reference state should be chosen at times $t = t_1, t_2, t_3$, etc. in place of the state $t = 0$. The total unwrapped phase change after re-referencing κ times will then be

$$\Delta\Phi_u(t,0) = \Delta\Phi_u(t,t_\kappa) + \sum_{k=2}^{\kappa} \Delta\Phi_u(t_k,t_{k-1}) + \Delta\Phi_u(t_1,0). \quad (7)$$

IMPLEMENTATION USING PIPELINE PROCESSOR

Pipeline processing essentially converts a two-dimensional image consisting of a 2-D array of pixel values into a one-dimensional stream of individual pixels. The pixel stream can be processed one pixel at a time by a series of specialised processing elements, and then transformed back into a 2-D image. At the beginning and end of each 1-D pipeline is a 2-D surface that is stored on a virtual surface image memory (VSIM). Pipeline processing has an important performance advantage over fixed-data-path, general-purpose image processing architectures, which process whole images as discrete frames. This advantage is derived from placing the specialised processing hardware at the particular point in the 1-D stream where it can perform its individual processing task on each pixel, without waiting for the entire frame to be processed. The processing hardware can be assembled in a variety of configurations, each optimised for a particular application, thereby creating an image pipeline.

The hardware used to implement the algorithm described in the previous section is a Datacube VME system, consisting of two 20MHz MV250 pipeline processor boards. The boards host a total of twelve dual ported 4Mb image memories (VSIM), an AP advanced processor module, and a mmNMAC2 convolver module. A Motorola 33MHz MVME167 single board computer configures the pipeline processing boards and schedules the data transfers. The LynxOs real-time Unix operating system was selected to enable processes to be prioritised, thus allowing deterministic algorithm run-times to be achieved.

A 60Hz EEV CAM17 synchronous camera with a 512×512 pixel CCD array is used to acquire the speckle interferograms. The lens used was a Nikon 50 mm camera lens. The camera has an 8-bit digital output that feeds directly into the AD digital input port of one of the pipeline boards. The CCD camera provides the master pixel clock and framing pulses; the pipeline processor is then configured as a slave to this external clock. 8-bit resolutions are used to represent most images, with 16 bit representations for $v(t)$, and 24 bits for $\Delta\Phi_u(t,0)$. Pipeline altering threads are used to construct pipes as required, thereby ensuring efficient use of the computing resources. Full details of the pipeline architecture are given in Ref. [10].

EXPERIMENTAL

The experiment described in this paper used a standard out-of-plane speckle interferometer with illumination and observation directions almost normal to the specimen surface, and with the reference wave introduced by means of a beamsplitter so as to emerge from the centre of the objective lens aperture [1] (see Figure 1 below). The light source was a 5 W frequency doubled YAG Verdi laser manufactured by Coherent, running at a power output of 0.6 W. Phase-shifting was carried out by means of a Pockels cell in the reference beam. A speckle shearing interferometer has also been constructed using a standard Michelson arrangement in which phase shifting is carried out by moving one of the two mirrors by means of a high voltage PZT (Burleigh PZ-81). The image processing steps implemented on the pipeline processor are, however, identical for both types of interferometer.

The sample consisted of a plate $150 \times 100 \times 1.5 \text{ mm}^3$, manufactured with the stacking sequence [0/90/0/0/90/0]. A double-layer of Teflon film (with dimensions $50 \times 50 \text{ mm}^2$) was included between the first and second plies to simulate the presence of a delamination crack. After curing, the sample was coated with titanium dioxide developer powder to increase the surface reflectivity and reduce speckle decorrelation. The plate was placed in a vacuum chamber with optical access provided by means of a polymethyl methacrylate window. The surface displacement field was measured as the pressure was reduced by 150 mbar over a period of 64 s. Re-referencing was carried out every 6.7 s.

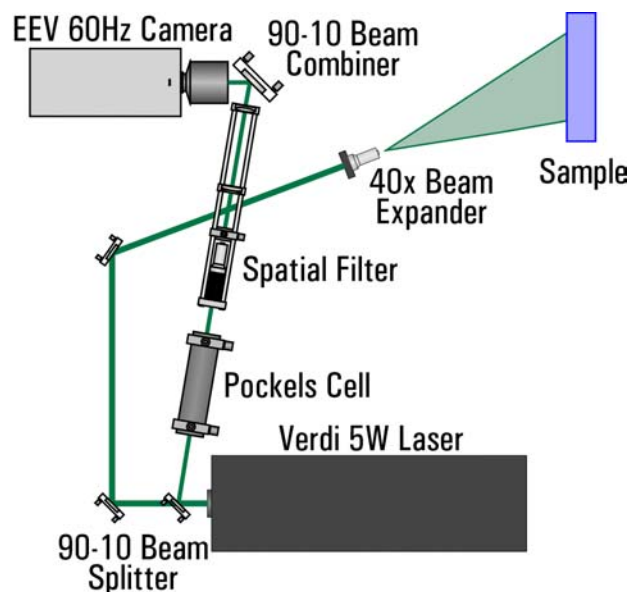


Figure 1: Optical arrangement for out-of-plane speckle interferometer.

Figure 2 shows the wrapped phase change map calculated by the pipeline processor over the course of the experiment. The grayscale colour map is such that $-\pi$ is represented by black, and $+\pi$ by white. The unwrapped phase map is represented on the monitor as a real-time colour coded image. In view of the difficulties of representing such images in a monochrome publication, we display the final unwrapped phase map as a surface mesh plot (Figure 3). This unwrapped phase map can be converted to the out-of-plane displacement component, $u_z(x, y)$, by multiplying by the constant $\lambda/4\pi = 42.3 \text{ nm rad}^{-1}$, where λ is the wavelength of the light used (532 nm) [1].

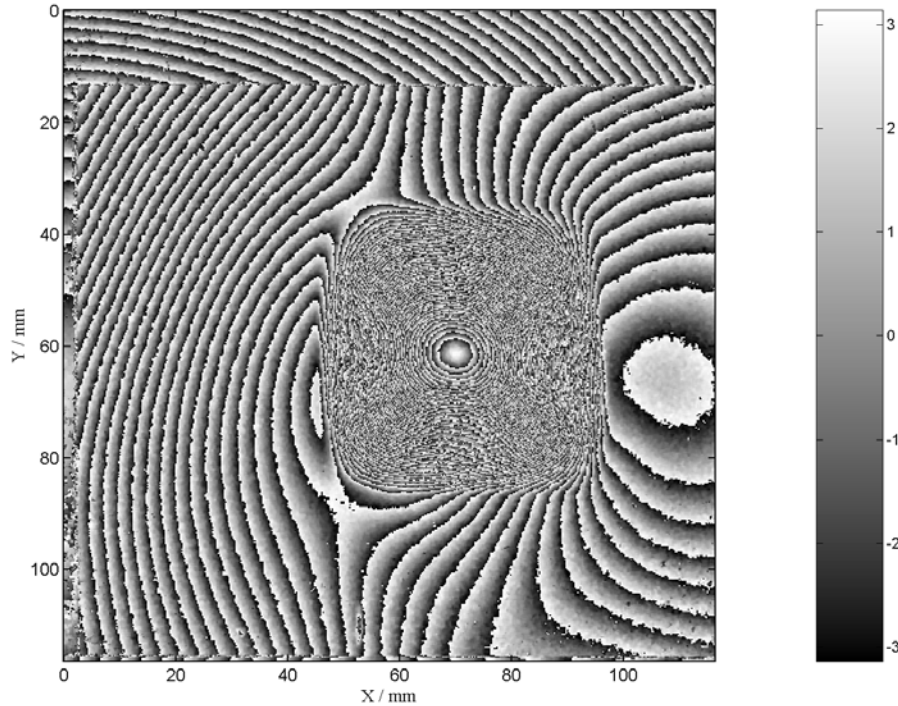


Figure 2: Wrapped phase map at end of test showing final deformation state of the carbon fibre sample.

CONCLUSIONS

This paper describes the first speckle interferometry analysis system which is capable of calculating and displaying maps of the displacement field in real time, i.e. at 15 frames s^{-1} . Data from 250,000 pixels are processed using a combination of temporal phase shifting and temporal phase unwrapping. Unwrapping errors due to low modulation pixels are effectively removed by convolution of the data with a 3×3 kernel, which therefore restricts spatial cross-talk to immediately adjacent pixels; each pixel cluster therefore behaves as an independent displacement sensor. In the case of spatial unwrapping, by contrast, each pixel is potentially influenced by every other pixel in the field of view. Increases in noise level in the measured displacement field due to speckle decorrelation are reduced by periodically re-referencing the phase map. In combination with a 24-bit representation of the speckle phase change, this allows specimen motion to be measured over an extended range (from -6.5 mm to $+6.5 \text{ mm}$ with respect to the initial position).

The performance of the system was demonstrated by high quality data calculated from a vacuum-loading test on a carbon-fibre composite panel containing a sub-surface delamination crack. The maximum measured displacement was $\sim 20 \mu\text{m}$, with an rms noise level of a few tens of nm, giving a signal-to-noise ratio of $\sim 1000:1$. This is significantly higher than values traditionally associated with the technique of speckle interferometry. Further research will involve the development of software to detect such defects automatically, and the use of inverse analysis techniques to quantify the flaw geometry [11].

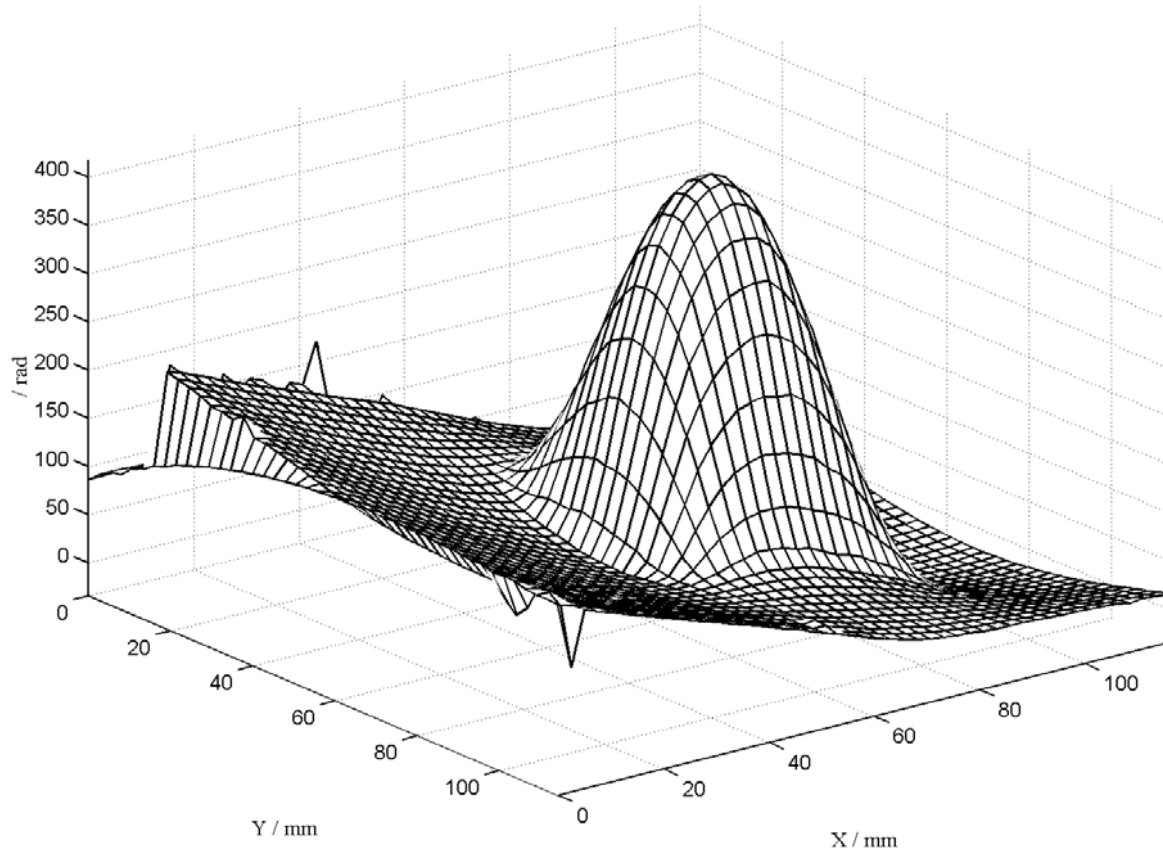


Figure 3: Result of temporal unwrapping of the phase map from Figure 2.

ACKNOWLEDGMENTS

The carbon fibre sample tested was manufactured by D. C. Panni. The work was funded by EPSRC under contract GR/M57835, and carried out in collaboration with British Aerospace Sowerby Research Centre.

REFERENCES

- [1] Jones, R and Wykes, C. (1983). *Holographic and Speckle Interferometry*. Cambridge University Press, Cambridge.
- [2] Bushman, T. (1989) *Proc. SPIE* 1162, 66.
- [3] van Haasteren, A. J. P. and Frankena, H. J. (1993). In: *Proc 2nd Intl. Workshop on Automatic Processing of Fringe Patterns*, pp. 417-422, Jüptner, W. and Osten., W. (Eds). Akademie Verlag, Berlin.
- [4] Ghiglia, D. C. and Pritt, M. D. (1998). *Two-dimensional phase unwrapping*. J. Wiley & Sons, New York.
- [5] Huntley, J. M. and Saldner, H. (1993) *Appl. Opt.* 32, 3047.
- [6] Colonna de Lega, X. (1997). *Processing of non-stationary interference patterns: adapted phase-shifting algorithms and wavelet analysis*. PhD thesis, EPFL Lausanne.
- [7] Joenathan, C. Franze, B. Haible, P. and Tiziani, H. J. (1998) *Appl. Opt.* 37, 2608.
- [8] Huntley, J. M., Kaufmann, G. H. and Kerr, D. (1999) *Appl. Opt.* 38, 6556.
- [9] Huntley, J.M. (1997) *Opt. Lasers Eng.* 26, 131.
- [10] Coggrave, C. R. and Huntley, J. M. (1999) *Proc SPIE* 3744, 464.
- [11] Panni, D. C. and Nurse, A. D. (submitted 2001) *Computers and Structures*.

